Stochastic Process Representation and Analysis of the Homogenizing Process in a Cement Plant

Ozaki, Kenji

Fukuoka, Masaki

Habata, Osamu

Proceedings of the 28th ISCIE International Symposium
on Stochastic Systems Theory and Its Applications
Kyoto, Nov. 14-16, 1996

Stochastic Process Representation and Analysis of the Homogenizing Process in a Cement Plant

Kenji Ozaki, Masaki Fukuoka, and Osamu Habata
Plant Engineering Group, Kawasaki Heavy Industries, Ltd.
1-1 Higashikawasaki-cho 3-chome, Chuo-ku, Kobe 650-91, JAPAN
ozaki_k@kow.khi.co.jp

Abstract

This paper presents a predicting method for variances of chemical composition fluctuations in a cement manufacturing plant using a stochastic representation for their fluctuations at the inlet of the plant and also using a dedicated transfer function of each element of the process. The theoretical calculation result of standard deviations is compared with the result measured in an actual plant.

1. Introduction

A typical process flow diagram of a cement manufacturing plant is shown in Fig. 1. In this plant, it is important to manage and control fluctuations of chemical compositions at the inlet of a kiln in order to obtain good quality of product and to maintain its stable operation. For manufacturing Portland cement, the following three moduli are used for their quality control:

Hydraulic modulus $HM = \dfrac{CaO}{SiO_2 + Al_2O_3 + Fe_2O_3}$,

Silica modulus $SM = \dfrac{SiO_2}{Al_2O_3 + Fe_2O_3}$, *and*

Iron modulus $IM = \dfrac{Al_2O_3}{Fe_2O_3}$

It is usual to keep these moduli of raw meal at a kiln inlet less than the predetermined value, for example, the standard deviation of HM should be less than 0.027[1]. For this purpose, a cement plant is exclusively equipped with dedicated installations such as homogenizing beds and blending silos for homogenizing raw material compositions. A raw material mixing control system is also provided to minimize variances which especially come from low frequency components of fluctuations. This control system is installed in the raw material grinding mill department and controls the mill inlet flow rates of four kinds of raw materials, which are limestone, clay,

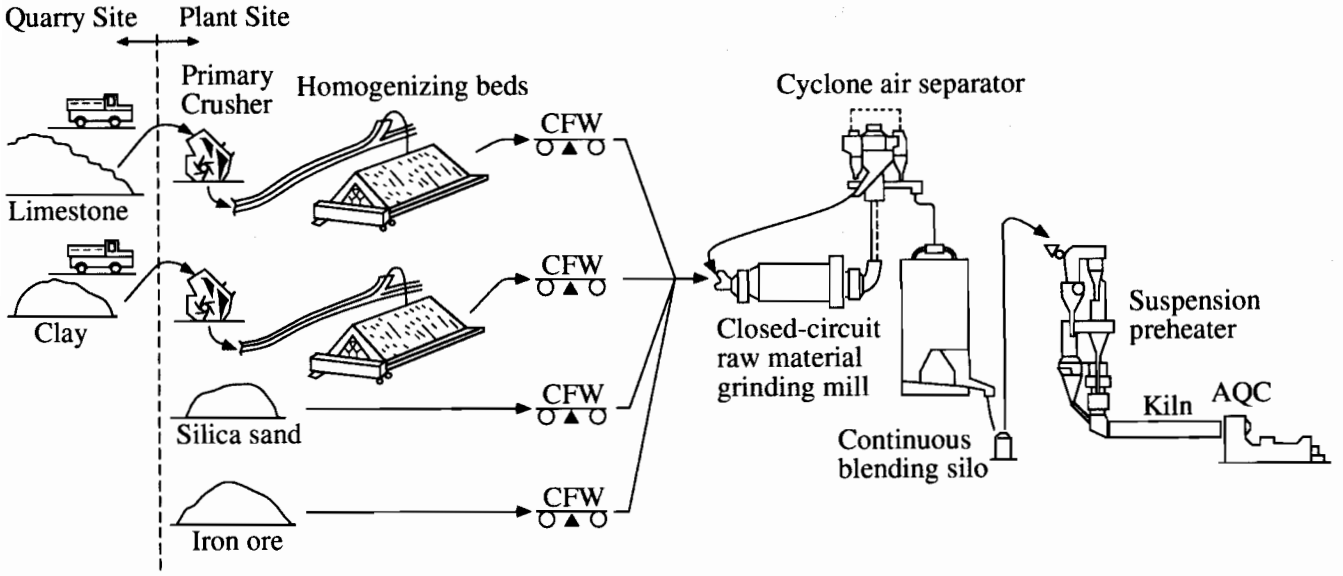

Fig.1 Typical process flow diagram of cement manufacturing plant.

silica sand, and iron ore, according to the result of an on-line chemical analysis of the mill outlet raw meal.

It would be very effective for planning a process during the initial stage of a project, if we could predict fluctuations of chemical compositions taking into account the effects of these installations. We cannot yet find any reports on such predicting methods. In this paper, the authors will present a theoretical approach to predict the decreasing degree of these fluctuations differing between two materials at the quarry site and at the kiln inlet. Then, the authors will show calculated results compared with measured results for an actual plant, by which it will be recognized that this method is fairy effective. Finally, the authors will present independent and combined homogenizing performance diagrams of these installations as a result of this analysis method.

In the following section, the concept for theoretical exploitation, assumptions for modeling and also examination results to justify these assumptions will be explained. The main point in this section is a proposition that the fluctuation process of chemical compositions at the inlet of a primary crusher can be represented by the product of two stochastic variables, one being a static stochastic variable having statistical characteristics derived from chemical analysis results for boring samples and the other one being a semirandom telegraph signal representing the dynamic characteristics of fluctuations. If we use this method, the fluctuation process can be made equivalent to the stochastic process of a Gausian white noise passing through a first order shaping filter.

In the third section, the transfer functions which represent the homogenizing effects of installations, such as homogenizing beds, raw material grinding mills, and blending silos, and also of a raw material mixing control system will be presented. As a result of analysis in these two sections, the composition variance at the kiln inlet, which is our main objective to predict, can be expressed by the following equation:

$$\sigma_{ij}^2=\frac{1}{2\pi}\int_{-\infty}^{\infty}\Phi_{ij}(\omega)\cdot|G_{HB}(j\omega)\cdot G_{GM}(j\omega)\cdot G_{BS}(j\omega)|^2 d\omega \cdots (1)$$

In the fourth section, diagrams which express the decrease of standard deviation at the outlet of each installation will be presented and the calculation result will be compared with the result of actual measurement. The authors will also make suggestions for the possibility of an effective planning method for several installations using these diagrams.

2. Concept of Modeling

Raw materials for cement manufacturing, in general, are limestone, clay, silica sand, and iron ore. As shown in Fig.1, the first two materials are excavated at the quarry site, while the other two materials are normally brought directly to each storage from other places. The two major excavated materials are put into a primary crusher, transported to the plant site, and then piled up in layers on each homogenizing bed, which has the primary homogenizing function. Then the four materials are mixed and fed to the grinding mill by constant feeders. After being ground under mixing effect, the product, which we call "raw meal", is fed to the blending silo where the raw meal is finally homogenized by blowing air into the silo.

2-1. Assumption for Modeling

The following assumptions are introduced for modeling;

(a). Static variations of chemical compositions of the major components, which are CaO in limestone, SiO_2 in clay, SiO_2 in silica sand, and Fe_2O_3 in iron ore, are expressed as normal distributions with sample means and sample variances calculated from the boring data.

(b). Variations of secondary components of each material are expressed respectively by a first-order regression formula with the variation of each major component.

(c). Time-domain fluctuations of raw materials at the inlet of the plant are each approximated by a stochastic process equivalent to a Gausian white noise passing through a first order shaping filter with a time constant T_{Mj}.

(d). Homogenizing effects in homogenizing beds, grinding mills, and blending silos can be characterized by linear time-invariant models and have the same characteristics for all the raw materials.

[Nomenclature]:

a_{ij} : weight percentage of i-th component of j-th raw material

x_j : mixing ratio of j-th material

y_i : weight percentage of i-th component of raw meal

$\boldsymbol{A} = [a_{ij}]$: raw material composition matrix

$\bar{\boldsymbol{y}} = \bar{\boldsymbol{A}} \cdot \bar{\boldsymbol{x}}$, $\bar{\boldsymbol{y}} = [\bar{y}_1, \bar{y}_2, \bar{y}_3, \bar{y}_4,]^T$, $\bar{\boldsymbol{x}} = [\bar{x}_1, \bar{x}_2, \bar{x}_3, \bar{x}_4,]^T$ where $\bar{}$ denote the values in steady state.

σ_{ij} : standard deviation of i-th component of j-th raw material

α_{ij} : regression coefficient between i-th and major components

$\boldsymbol{R} = [\alpha_{ij}]$: regression coefficient matrix

β_{ij} : intercept of regression line of $\hat{a}_{ij}$ on major components

$\Phi_{ij}(\omega)$: power spectrum function of i-th components of j-th material at the plant inlet

$G_{HB}(s)$: transfer function of homogenizing bed

$G^{O}_{GN}(s)$: transfer function of grinding mill without raw material mixing control

$G^{C}_{GM}(s)$: transfer function of grinding mill with mixing control

$G_{BS}(s)$: transfer function of blending silo

$G^{*}_{C}(z)$: pulse transfer function of raw material mixing control system

2-2. Examination of Assumptions

(a). Statistical distributions of major components

Frequency distributions of major components which are CaO% in limestone and SiO_2% in clay are respectively shown in Figs. 2 and 3. These distributions have been calculated from the boring data on four districts in three countries. The component of CaO in limestone has a distribution close to the Rayleigh distribution with a limited value of 56% which corresponds to the CaO content in pure limestone. On the other hand, SiO_2% in clay is close to a normal distribution as a result of the fact that clay is, in general, composite material with several mineral components of clay such as Kaolinite and several foreign materials including quartz. This fact is a manifestation of the " central limit theorem" .

In the following analysis, we approximate these distributions with normal distributions, taking account of objective materials being homogeneously made from several raw composites and also for convenience for theoretical exploitation.

(b). Regression between major and secondary components

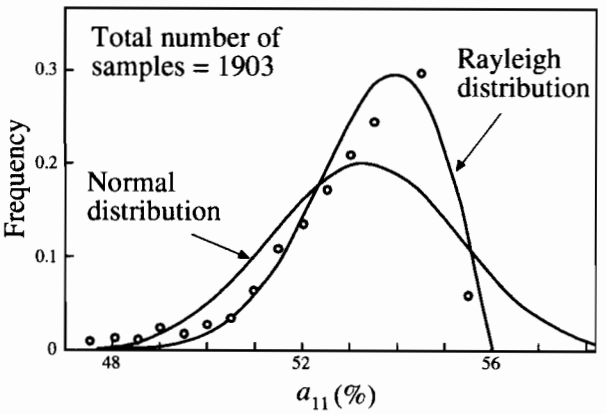

Fig.2 Frequency distribution of CaO% in limestone.

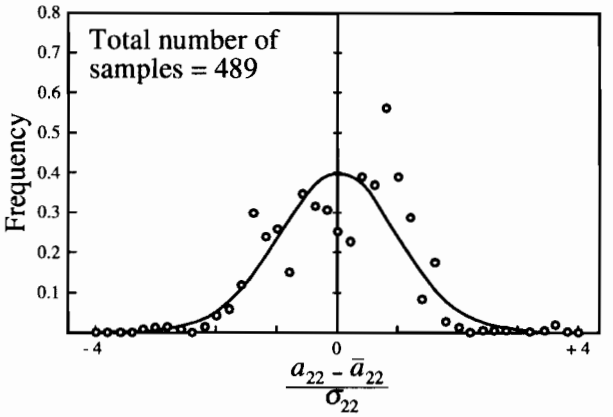

Fig.3 Nomarized frequency distribution of SiO_2% in clay .

It can be expected that there is strong correlation between components of raw materials because, for example in clay, several composites coexist as a crystal structure. Table 1 shows the result of regression analysis between components of limestone and clay calculated from the boring data on one district which include 231 samples of limestone and 199 samples of clay. Regression results for secondary components of which the contents are more than 5% keep their multiple correlation coefficients (R) greater than 0.80 and their standard deviations of errors between regression results and real sample data are within 11% of each mean contents. Consequently, they can be expressed by first-order regression calculations incorporating the major components.

Table 1 Regression analysis results

		Mean content	Correlation coefficient				Regression results			
		(%)	CaO	SiO_2	Al_2O_3	Fe_2O_3	β	α	R	σ_R
Limestone	CaO	50.3	1.0	-.98	-.55	-.46	—	—	—	—
	SiO_2	6.18		1.0	.41	.32	67.65	-1.22	.95	.684
	Al_2O_3	1.26			1.0	.88	7.66	-.127	.30	.478
	Fe_2O_3	0.57				1.0	2.90	-.047	.21	.220
Clay	CaO	24.2	1.0	-.99	-.92	-.94	54.06	-.977	.99	.872
	SiO_2	30.5		1.0	.89	.91	—	—	—	—
	Al_2O_3	12.0			1.0	.96	2.22	.320	.80	1.36
	Fe_2O_3	5.03				1.0	.907	.135	.83	.510

$$R^2 = \frac{\sum(\text{Estimated data} - \text{Sample mean})^2}{\sum(\text{Sample data} - \text{Sample mean})^2}$$

σ_R = Standard deviation of error between regression result and real sample data

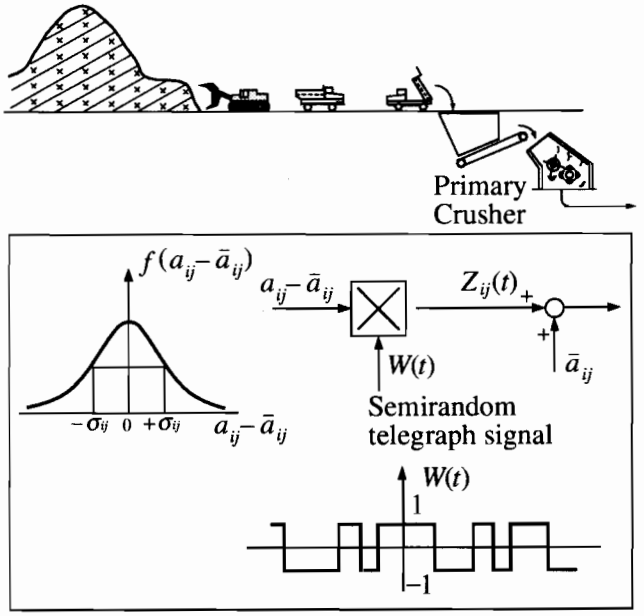

Fig.4 Stochastic representation of composition fluctuation.

(c). Fluctuation characterizing at the inlet of the plant

In order to predict the standard deviations of composition fluctuations at the kiln inlet using Equation (1), it is necessary to specify the time-domain characteristics of their fluctuations at the inlet of the primary crusher in addition to static characteristics mentioned above. Raw materials of limestone and clay, in general, are periodically transported using dump trucks from the quarry site to the primary crusher. Consequently, as illustrated in Fig. 4, we may say that the stochastic process of composition fluctuations at the inlet of the crusher can be expressed as the product of a static stochastic variable $a_{ij} - \bar{a}_{ij}$ and a semirandom telegraph signal W(t) with a mean zero crossing time interval of $2/T_{Mj}$ [2]. As these stochastic variables are mutually independent, we obtain the following two results for these variables $Z_{ij}(t) = (a_{ij} - \bar{a}_{ij})\, W(t)$;

$$\begin{aligned} R_{ij}(\tau) &\equiv E\left[\{Z_{ij}(t) - \bar{a}_{ij}\}\{Z_{ij}(t-\tau) - \bar{a}_{ij}\}\right] \\ &= E\left[(a_{ij} - \bar{a}_{ij})^2\right] E\left[W(t) \cdot W(t-\tau)\right] \\ &= \sigma_{ij}^2 \cdot \exp\left(\frac{-|\tau|}{T_{Mj}}\right) \quad \cdots (2) \end{aligned}$$

$$\Phi_{ij}(\omega) = \frac{2T_{Mj}\sigma_{ij}^2}{1 + (\omega T_{Mj})^2} \quad \cdots (3)$$

On the other hand, W(t) is also a kind of expression for a Poisson arrival process, and so the time constant T_{Mj} corresponds to the mean arrival time interval of dump trucks. Equations (2) and (3) show that this process is equivalent to the stochastic process of a Gausian white noise passing through a shaping filter.

3. Transfer Functions of Processes

We introduce transfer functions as follows for a representative cement plant which consists of chevron type homogenizing beds, a closed-circuit ball mill with an air separator, and continuous type blending silo with a mixing chamber at the lower part of the silo. The transfer functions of other types of processes have been introduced in another report by the authors[3].

3-1. Chevron Type Homogenizing Bed

This installation is composed of stacking machines, reclaiming machines, and stock piles for each raw material. With stacking machines, raw materials coming from the quarry site are piled up in separate layers all along the stock pile, so that the stock piles have multi-layers of raw materials. After the N-th layers have been piled up, the bridge type reclaiming machine excavates the raw materials in the direction perpendicular to the stacked layers. The decreasing ratio of variances of each material composition near the center of the pile can be theoretically expressed as the following if the speed of stacking machine is negligibly small as compared with the material

feeding speed and the correlation function of composition fluctuation of feeding material is expressed by Equation (2).

$$\frac{\sigma_{ij}^2(out)}{\sigma_{ij}^2(in)} = \frac{1}{N} + \frac{1}{N}e^{-x} + \frac{1}{N^2(1-e^{-x})^2}\{N(1-e^{-2x}) - 2(1-e^{-Nx})\} \quad \cdots (4)$$

where T_L is stacking period and $x = T_L / T_M$.

If we consider only the decreasing ratio of variance, it can be approximated to the gain characteristics of the following first-order lead-and-lag transfer function.

$$G_{HB}(s) = \frac{1 + \frac{\sqrt{N}}{2}T_L \cdot s}{1 + \frac{N}{2}T_L \cdot s} \quad \cdots (5)$$

The error between these two equations in the case of a typical layer number $N = 400$ is shown in Fig. 5.

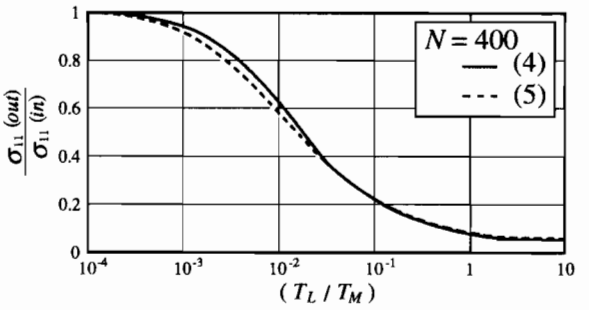

Fig.5 Variance decreasing characteristics expressed by Equations (4) and (5).

3-2. Closed-circuit Ball Mill

(a). Transfer function without mixing control

The authors have reported the transfer function derived from mass balance and surface balance equations using actual measurement results for a residence time distribution[4]. When examining the decreasing ratio of fluctuations, we may take account of only mass balance and we can obtain the following transfer function.

$$G_{GM}^{O}(s) = \frac{1}{(1 + L_C)(1 + T_B s)^5 - L_C} \quad \cdots (6)$$

where $5 \times T_B$ is the mean residence time of the ball mill itself and L_C is a circulation ratio (= return flow rate / product flow rate in steady state).

(b). Transfer function with mixing control

The raw material mixing control system, in general, is composed of sampling devices periodically taking out raw meal from the outlet transportation line, an X-ray spectrometer, a control computer, and constant feeders for four raw materials. The control computer receives analysis results from the spectrometer at control intervals and adjusts the mixing ratios of the four materials by sending set point signals to each constant feeder. The control block diagram is shown in Fig. 6. The closed-circuit ball mill has a high degree of delay and also pure delays such as the time taken from the transportation line to the sampler and spectrometer analyzing time. For this reason, we approximate the objective with a transfer function such as $\frac{f_o e^{-Ls}}{1 + T_o s}$. In our control algorithm[5], the discrete time operator $G_C^*(z)$ equivalent to the pulse transfer function of a PI controller with a Smith compensator for pure delay is applied to each measured HM, SM, and IM to set corrective targets for these moduli and then the mixing ratios for the next step are calculated against these new targets.

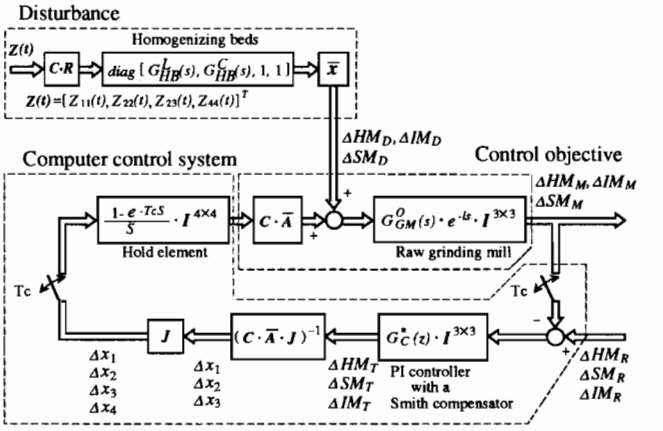

Fig.6 Block diagram of a raw mixing control system.

$$\boldsymbol{C} = \begin{bmatrix} C_{11} & C_{12} & C_{12} & C_{12} \\ 0 & C_{22} & C_{23} & C_{23} \\ 0 & 0 & C_{33} & C_{34} \end{bmatrix}, \quad C_{11} = \frac{1}{\bar{y}_2 + \bar{y}_3 + \bar{y}_4} \quad C_{12} = -\overline{HM} \cdot C_{11}$$

$$C_{22} = \frac{1}{\bar{y}_3 + \bar{y}_4} \quad C_{23} = -\overline{SM} \cdot C_{22}$$

$$C_{33} = \frac{1}{\bar{y}_4} \quad C_{34} = -\frac{1}{\bar{y}_3}$$

$$\boldsymbol{J} = \begin{bmatrix} 1 & 0 & 0 \\ 0 & 1 & 0 \\ 0 & 0 & 1 \\ -1 & -1 & -1 \end{bmatrix}, \quad \boldsymbol{R} = \begin{bmatrix} 1 & \alpha_{12} & \alpha_{13} & \alpha_{14} \\ \alpha_{21} & 1 & 1 & \alpha_{24} \\ \alpha_{31} & \alpha_{32} & \alpha_{33} & \alpha_{34} \\ \alpha_{41} & \alpha_{42} & \alpha_{43} & 1 \end{bmatrix}, \quad \bar{\boldsymbol{A}} = [\bar{a}_{ij}]$$

$$G_C^*(z) = \frac{G_{C1}^*}{G_{C2}^*},\quad G_{C1}^*(z) = K_P\left(1 + \frac{T_c}{T_i}\frac{z^{-1}}{1-z^{-1}}\right)(1-hz^{-1})(1-z^{-1})$$

$$G_{C2}^*(z) = (1-hz^{-1})(1-z^{-1}) + f_o K_P(1-z^{-k})z^{-1}\left[\left(1-\frac{T_o}{T_i}\right)(1-h)(1-z^{-1}) + \frac{T_c}{T_i}(1-hz^{-1})\right]$$

where, T_c is the sampling period, K_P and T_i are parameters of the PI controller, and $k = L / T_c$, $h = \exp(-T_c / T_o)$.

3-3. Continuous Type Blending Silo

In this installation, the dynamic behavior of raw meal can be approximated with a continuously stirred tank reactor model which has intermediate behavior between piston flow and perfect mixing. As actual measurement results for the residence time distribution, the transfer function of this installation can be expressed as follows, neglecting pure delay:

$$G_{BS}(s) = \frac{1}{\left(1 + \frac{V}{4Q}s\right)^4} \quad \cdots (7)$$

where V is the volume of the mixing chamber and Q is the flow rate of raw meal.

Using these proposed transfer functions of several installations and Equation (1), we can now calculate the standard deviation for each component at the inlet of the kiln.

4. Calculation Results

The overall schematic block diagram which summarizes the descriptions in the second and the third section is shown in Fig. 7. An example of a set of transfer functions with numerical constants is also shown in this figure. These constants were calculated for the installations of ENFIDA plant in Tunisia. The

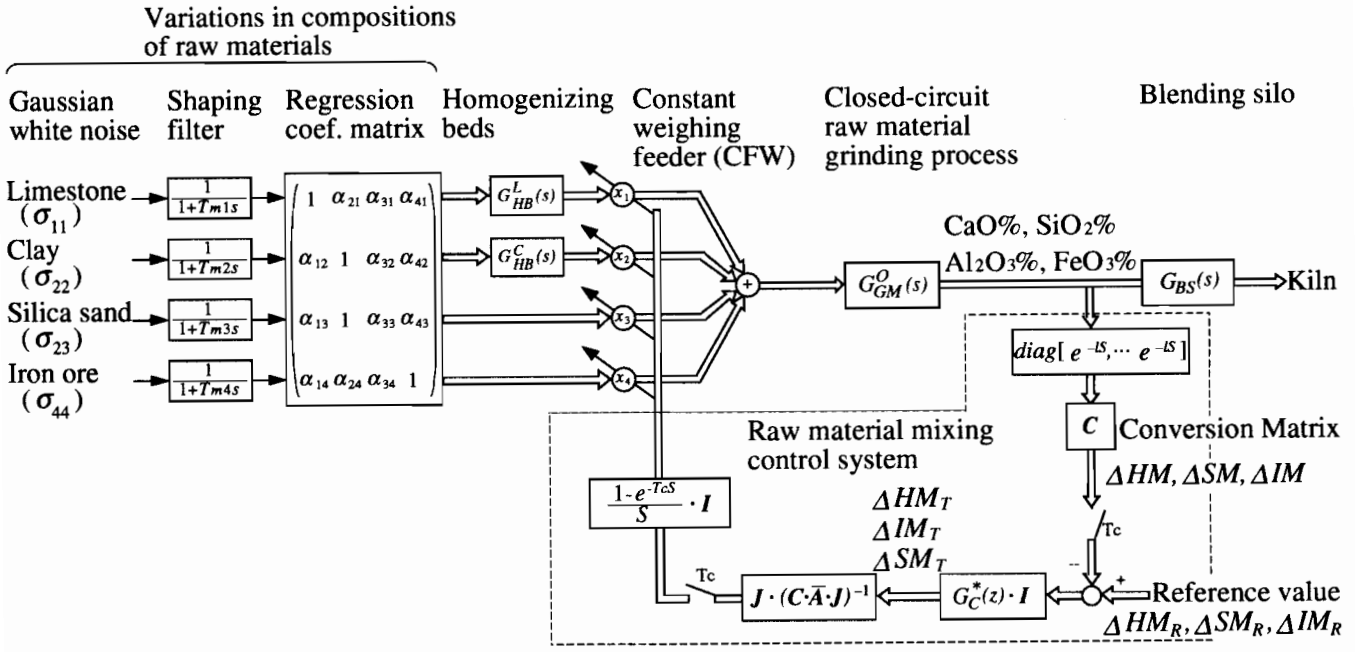

	Variations in compositions of raw materials	Homogenizing bed	Closed-circuit raw grinding mill		Blending silo
			without mixing control	with mixing control	
Example of ENFIDA	$\Phi_{11}(\omega) = \frac{2\times0.067\times(2.46)^2}{(1+0.067\omega)^2}$ $\Phi_{22}(\omega) = \frac{2\times0.067\times(2.6)^2}{(1+0.067\omega)^2}$	$G_{HB}^L(s) = \frac{1+0.73s}{1+14.76s}$ $G_{HB}^C(s) = \frac{1+0.408s}{1+5.74s}$	$G_{GM}^O(s) = \frac{1}{4(1+0.038s)^5 - 3}$	$J\cdot(C\cdot A\cdot J)^{-1} = \begin{pmatrix} 0.198 & 0.070 & -0.124 \\ -0.124 & -0.082 & 0.184 \\ -0.055 & 0.026 & -0.021 \\ -0.019 & -0.014 & -0.038 \end{pmatrix}$ $Tc = 1$(hr) $Kp = 0.2$ $Ti = 0.8$(hr) $To = 0.7$(hr) $L = 1$(hr)	$G_{BS}(s) = \frac{1}{(1+5.7s)^4}$

Fig.7 Overall schematic block diagram of homogenizing processes and their examples.

time constant T_{Mj} of the shaping filter is calculated as twice the mean arrival time interval of dump trucks because limestone and clay are put into the same crusher with same period, that is, 0.067h for limestone and clay.

4-1. Diagrams for Fluctuation Decreasing Performance

Two examples of diagrams of the captioned performance are shown in Figs. 8-1 and 8-2. The former is independent performance of each installation and the later is combined performance calculated for cascade connection of several installations, which shows the decreasing ratio between the inlet of the plant and the outlet of the last installation. Further, the values of standard deviation for CaO%, SiO_2%, HM, and SM are shown in the schematic flowchart(Fig. 9). Using these figures, we arrive at the following features to be noted especially when planning these installations for homogenizing purpose;

(1). The performance of the grinding mill is less important in itself than that of the other installations, but if a raw material mixing control system is installed, the low-frequency performance will be much improved, and large variance decrease can be expected. According to the authors' calculation, the standard deviation for HM at the outlet of the raw mill with control is about one-third

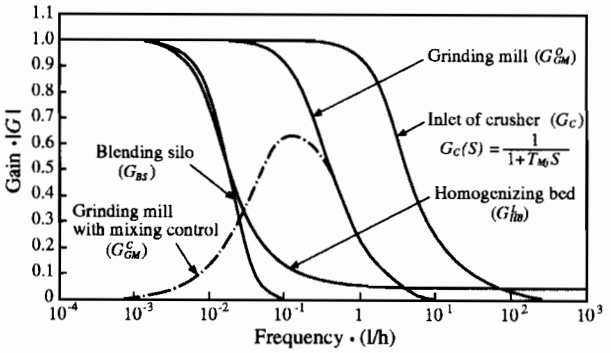

Fig.8-1 Individual process performance.

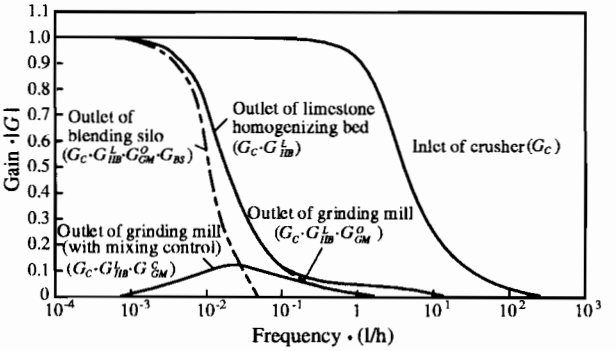

Fig.8-2 Combined performance.

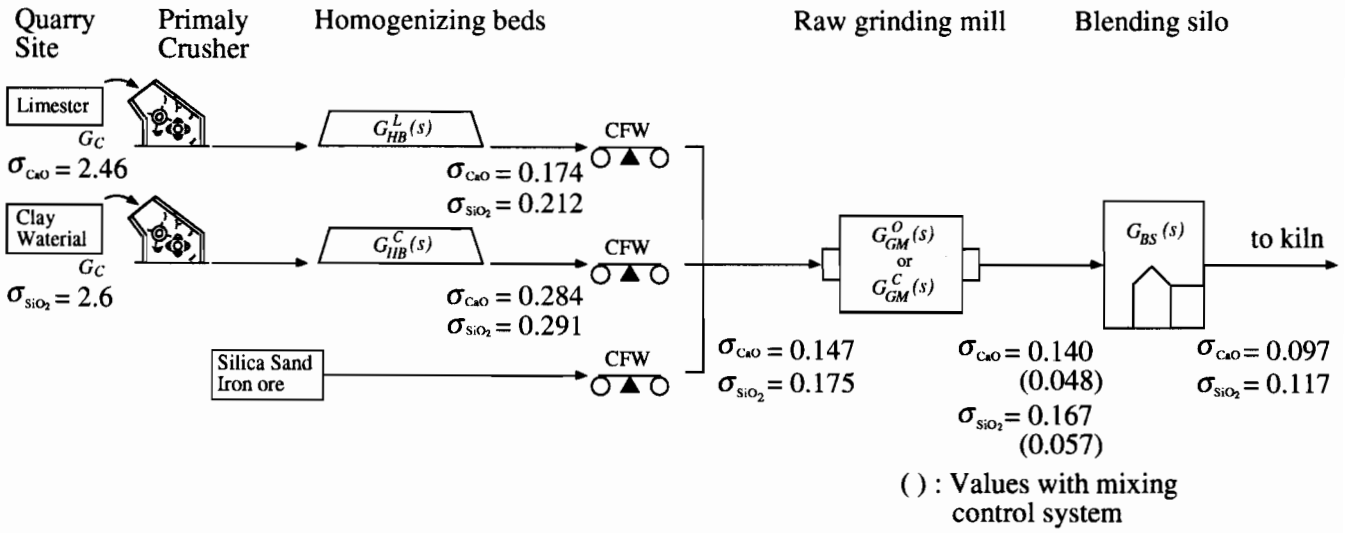

σ_{HM} and σ_{SM} for mixture of four materials (supposed)	$\sigma_{HM} = 0.390$ $\sigma_{SM} = 0.442$	$\sigma_{HM} = 0.029$ $\sigma_{SM} = 0.036$	$\sigma_{HM} = 0.028(0.010)$ $\sigma_{SM} = 0.034(0.012)$	$\sigma_{HM} = 0.019$ $\sigma_{SM} = 0.023$
	Inlet of crusher	Inlet of mill	Outlet of mill	Outlet of silo

Fig.9 Standard deviations at each point of plant.

of that without control. On the other hand, this ratio is almost one half by actual measurement results[5]. These two figures show that this calculation method gives us fairly good results.

(2). From combined performance, it can be said that the performance of an installation is strongly affected by the characteristic of the preceding installation. Consequently, we must be careful not to apply variance reduction data on an existing plant to another plant only by simple multiple calculations; it is necessary to calculate it as shown in this paper, taking account of the frequency responses of the constituent installations especially the preceding installations.

(3). The performances of the homogenizing bed and the blending silo are similar. On the other hand, by the calculation for this example, the ratio of standard deviation decrease by the blending silo is about 1 / 1.38 (72%) when the raw material mixing control system is installed. This figure is much less than the independent performance ratio of 1 / 16.45(6%). This fact suggests the possibility that we can replace one of these installations with another type of installation only with storage function, which is more economical.

4-2. Comparison with Actual Measurement Results

The authors have taken 52 samples of raw meal at the kiln inlet during 6 days' operation by cutting off mixing control in the ENFIDA plant mentioned earlier. The standard deviation of HM calculated with these samples was 0.0142 against the theoretical calculated value of 0.0190. This result shows that it is fairly good even though we had made several assumptions.

5. Concluding Remarks

In this paper, the authors have presented an effective analyzing method for the homogenizing process in a cement plant, applying a stochastic process representation for fluctuations of chemical compositions of raw materials and also using several transfer functions which were theoretically or experimentally derived. Using this method, accordingly, it enables us to make a systematic planning of such a process including the raw material mixing control system to realize an optimum combination of the constituent installations and the control system. The authors have also presented the structure of the mixing control system as a linear multivariable control system using transfer function matrixes for a control objective and stochastic disturbances. This structure shows that the raw material mixing control system is a kind of stochastic multivariable control system. It offers the possibility of applying linear multivariable adaptive control in order to minimize variances of three moduli, such as the hydraulic modulus, silica modulus, and iron modulus. The authors report about it in the near future.

6. References

[1] Committee on chemical analysis of the cement association of Japan: Investigation on the utilization of fluorescent X-ray analyzer in the cement industry in Japan, 146(1978)

[2] Papoulis, A. : Probability, random variables and stochastic processes, McGraw-Hill(1965)

[3] H.Sugimoto, K.Ozaki et al. : Development of generalized homogenizing process analysis and synthesis method in cement industry-1st and 2nd reports-, Kawasaki Technical Review 90, 95(1985, 1987)

[4] K.Ozaki et al. : Analysis and control of closed-circuit grinding system, Kawasaki Technical Review 59(1975)

[5] H.Sugimoto, K.Ozaki et al. : Computer control technique for cement plants, Kawasaki Technical Review 64(1977)